Journal of Radioanalytical and Nuclear Chemistry (2020) 324:1405–1421
https://doi.org/10.1007/s10967-020-07182-w

Investigation of the deuteron induced nuclear reaction cross sections on lutetium up to 50 MeV: review of production routes for ^{177}Lu, ^{175}Hf and ^{172}Hf via charged particle activation

F. Tárkányi[1] · S. Takács[1] · F. Ditrói[1] · A. Hermanne[2] · R. Adam-Rebeles[2] · A. V. Ignatyuk[3]

Received: 28 February 2020 / Published online: 7 May 2020
© The Author(s) 2020

Abstract
In a systematic study of light charged particle induced nuclear reactions we investigated the excitation functions of deuteron induced nuclear reactions on natural lutetium targets. Experimental excitation functions up to 50 MeV on high purity ^{nat}Lu were determined using the standard stacked foil activation technique. High resolution off-line gamma-ray spectrometry was applied to assess the activity of each foil. From the measured activity direct and/or cumulative elemental cross-section data for production of ^{171,172,173,175}Hf, ^{171,172,173,174g,176m,177m,177g}Lu and ^{169}Yb radioisotopes were determined. The experimental data were compared to results of the TALYS theoretical code taken from the TENDL databases and results of our calculations using the ALICE-IPPE-D and the EMPIRE-D codes. No earlier experimental data were found in the literature. Thick target yields for the investigated radionuclides were calculated from the measured excitation functions.

Keywords Lutetium target · Deuteron irradiation · Hf, Lu and Yb radioisotopes · Cross section · Theoretical model calculation · Physical yield

Introduction

Presently, the proton induced reactions play major role in different applications due to simpler production of high energy/intensity proton beams, to low stopping-power, and to the relatively high cross sections of the reactions. The second most important light charged particle is deuteron, due to simple production of high intensity beam, the moderate stopping compared to heavier particles, relatively high cross sections, and to production of high intensity neutrons via break up. The activation cross sections of deuteron induced reactions are important for a wide variety of applications: isotope production, accelerator technology and material studies, thin layer activation (TLA) for wear studies.

A few decades ago the status of the database for deuteron induced reactions was relatively poor compared to that was available for proton induced reactions, and the quality of the theoretical descriptions was, even after several attempts for improvement, far from being acceptable. Therefore, we have started systematic study of activation cross sections of deuteron induced reactions in a broad international cooperation. The already reported, peer reviewed, investigations include around 640 reactions induced on 61 target elements: Be, B, C, N, Ne, Mg, Al, Si, Sc, Ti, V, Cr, Mn, Fe, Co, Ni, Cu, Zn, Ga, Ge, Kr, Sr, Y, Zr, Nb, Mo, Rh, Pd, Ag, Cd, In, Sn, Sb, Te, Xe, Cs, Ba, La, Ce, Pr, Nd, Sm, Eu, Gd, Tb, Dy, Er, Tm, Yb, Hf, Ta, W, Re, Os, Ir, Pt, Au, Hg, Tl and Pb. A significant part of the cross section data was reported for the first time. A systematic comparison with the results calculated with theoretical models allows conclusions on the predictivity of the different codes (ALICE-IPPE, EMPIRE, GNASH, TALYS, PHITS). The database was especially poorly populated for rare earths, due to more limited applications (compared to metals) and to the more complicated target preparation. In the present work we report on cross section data on natural lutetium (missing in our rare earth list), for which no experimental data are available in the literature.

✉ F. Ditrói
ditroi@atomki.hu

[1] Institute for Nuclear Research (ATOMKI), Debrecen, Hungary

[2] Cyclotron Laboratory, Vrije Universiteit Brussel (VUB), Brussels, Belgium

[3] Institute for Physics and Power Engineering, Obninsk, Russian Federation

Preliminary results were presented in the RANC-2016 conference [1]. The activation cross section data for production of ^{172}Hf on natural hafnium were published in our paper investigating production routes of the ^{172}Hf/^{172}Lu generator and ^{169}Yb [2].

Experiment and data evaluation

Target preparation

Due to limited beam time only one stack was prepared containing 25 high purity lutetium foils (Goodfellow) with natural isotopic composition and nominal thickness of 110 µm interleaved with 27 µm aluminum beam monitor foils (Goodfellow). The aluminum foils were evenly distributed in the stacks to cover the full energy range. The number of target atoms was determined by measuring the surface and weight of the individual foils.

Irradiation

The stacks were irradiated at the Cyclone 90 cyclotron of Université Catholique in Louvain la Neuve (LLN) Belgium using our standard Faraday-cup type target holder. Irradiation took place with a constant 100 nA beam current for 40 min. The primary beam energy was determined by the settings of the cyclotron. Both the beam energy and intensity were corrected on the basis of the detailed re-measured and analyzed excitation function of the ^{nat}Al(d,x)^{22,24}Na monitor reactions compared to the latest recommended values [3]. The recoil fragments from the Al targets were corrected by ^{22,24}Na activities measured in the Lu samples positioned behind Al in the stack ("corrected" in Fig. 1), but the results without recoil correction are also presented for comparison ("uncorrected" in Fig. 1). As can be seen in Fig. 1 for the ^{27}Al(d,x)^{24}Na monitor reaction, the agreement is very good over the whole energy range without any correction in energy or beam current. The main parameters of the experiment and the methods of data evaluations with references are summarized in Table 1.

The activity produced in the target and monitor foils was measured non-destructively (without chemical separation) at VUB-Brussels cyclotron laboratory with a high resolution off-line HPGe gamma-ray spectrometer coupled to a Canberra-GENIE acquisition system. The evaluation of the measured spectra and the determination of the net counts in the gamma-ray peaks were made by the peak fitting algorithm included in the GENIE software package and by the interactive Forgamma software [4]. The irradiated foils were measured at three different times after the EOB (End of Bombardment). The first acquisition started 7.4 h after the EOB due to the initial high activity and transport from the irradiation to the measurement site.

Direct and/or cumulative elemental cross section data were determined from the measured activity of the reaction products. Some of the radionuclides formed are the result of cumulative processes where decay of parent nuclides or metastable state contributes to the production process. The used nuclear data (half-lives and gamma branching ratios), the possible contributing reactions and their Q-values are shown in Table 2. The listed Q-values refer to formation of the ground state. The energy degradation as a function of penetration of the bombarding particles in the stack was determined by a stopping calculation and based on incident energy according to the monitor reaction. The uncertainty

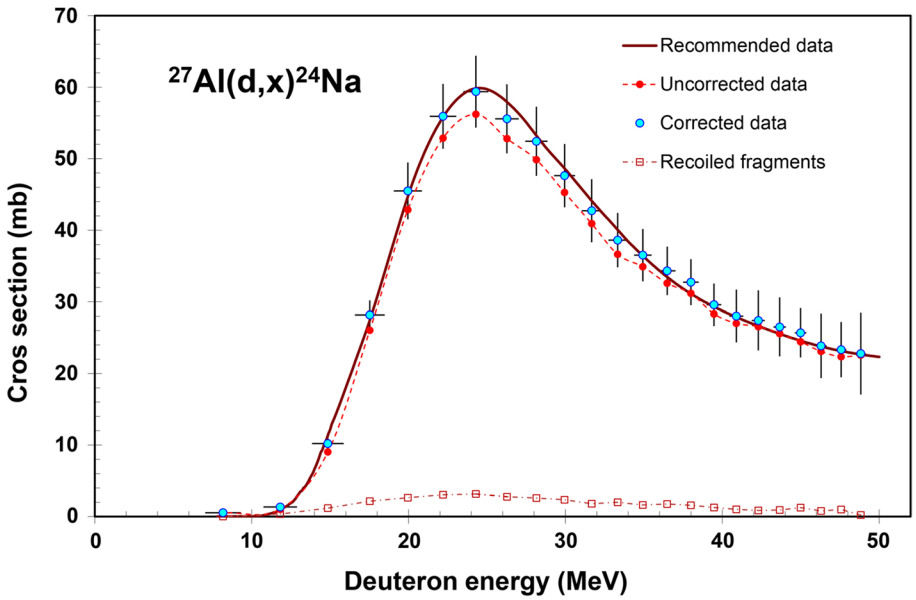

Fig. 1 Application of monitor reactions for determination of deuteron beam energy and intensity

Table 1 Main parameters of the experiment and the methods of data evaluation

Experiment		Data evaluation	
Incident particle	Deuteron	Gamma spectra evaluation	Genie 2000 [5], Forgamma [4]
Method	Stacked foil	Determination of beam intensity	Faraday cup (preliminary) Fitted monitor reaction (final) [6]
Target stack and thicknesses	25 blocks of Lu (110.42 μm), Al (26.96 μm)	Decay data	NUDAT 2.7 [7]
Number of target foils	25	Reaction Q-values	Q-value calculator [8]
Accelerator	Cyclone 90 cyclotron of Université Catholique in Louvain la Neuve (LLN) Belgium	Determination of beam energy	Andersen-Ziegler (preliminary) [9] Fitted monitor reaction (final) [10]
Primary energy	50 MeV	Uncertainty of energy	Cumulative effects of possible uncertainties
Irradiation time	40 min	Cross sections	Elemental cross section
Beam current	110.42 nA	Uncertainty of cross sections	Sum in quadrature of all individual contributions [11]
Monitor reaction, [recommended values]	^{27}Al(d,x)^{22,24}Na [10]	Yield	Physical yield [12, 13]
Monitor target and thickness	Al (26.96 μm)	Theory	ALICE-IPPE-D [14], EMPIRE-II-D [15], TALYS 1.9 in (TENDL-2017, 2019) [16, 17]

Detector HPGe

γ-spectra measurements 3 series

Cooling times (h) 7.4–12.5, 44.3–54.5 and 290.5–486.0

on each experimental cross section data point was estimated by taking the square root of the sum in quadrature of all individual contributing error components, supposing equal sensitivities for the linearly contributing different parameters appearing in the formula: counting statistics 1–18%, detector efficiency 5–7%, gamma intensities 1–3%, effective target thickness 5% and beam current 7%. The contributions on the uncertainties of non-linear parameters were neglected (time, half-life, etc.). Taking into account the cumulative effects of possible uncertainties of the primary incident energy, of the thickness and homogeneity of the different targets and of the energy straggling the uncertainty on the median energy in each foil varies between ± 0.3 and ± 1.1 MeV from the first to the last.

Model calculations

The updated ALICE-IPPE-D [14] and EMPIRE-D [15] codes were used to analyse the experimental results. As described in detail in our earlier publications, Tárkányi et al. [19] and Hermanne et al. [20], these modified codes were developed to assure a better description of deuteron induced reactions. In the standard versions of the codes a simulation of direct (d,p) and (d,t) phenomena is included through an energy dependent enhancement factor for the corresponding transitions. The parameters were taken as described in Belgya et al. [21]. The theoretical data from the TENDL-2017, Koning 2017 [22] and the TENDL-2019 [17] libraries (based on the modified TALYS 1.9 code, Koning 2017 [23] and standard input parameters) was also used for a comparison. For most activation products also the values for the TENDL-2015, calculated with an earlier TALYS version are shown in order to demonstrate only marginal differences between them.

Results

Cross sections

The cross sections for all the reactions studied are shown in Figs. 2, 3, 4, 5, 6, 7, 8, 9, 10, 11, 12 and 13 and the numerical values are collected in Tables 3, 4 and 5. For completeness we have included also the cross section data for production of ^{172}Hf, measured in present study and reported earlier in [2]. Although all activation products except ^{177}Lu are formed in reactions on both stable Lu isotopes, remarkable surplus of ^{175}Lu over ^{176}Lu (97.4/2.6) results in dominance of the reactions on ^{175}Lu and in presence of a single peak in the measured excitation functions.

Table 2 Decay characteristics of the investigated activation products (primary evaluation peaks are bold) [8, 18]

Nuclide decay E (level)	Half-life	E_γ (keV)	I_γ (%)	Contributing reaction	Q-value (keV)
^{175}Hf	70 d	**343.40**	84.0	^{175}Lu(d,2n)	− 3690.83
ε: 100%		433.0	1.44	^{176}Lu(d,3n)	− 9978.8
^{173}Hf	23.6 h	**123.675**	83	^{175}Lu(d,4n)	− 18,903.3
ε: 100%		139.635	12.7	^{176}Lu(d,5n)	− 25,191.3
		296.974	33.9		
		311.239	10.7		
^{172}Hf	1.87 y	114.061	2.6	^{175}Lu(d,5n)	− 25,984.2
ε: 100%		**125.812**	11.3	^{176}Lu(d,6n)	− 32,272.2
^{171}Hf	12.1 h	**347.20**	6(150*)	^{175}Lu(d,6n)	− 35,026.4
		662.20	10(266*)	^{176}Lu(d,7n)	− 41,314.4
^{177m}Lu	160.44 d	105.3589	12.4	^{176}Lu(d,p)	4848.324
β-: 78.60%		112.9498	21.9		
		128.5027	15.6		
IT: 21.4%		153.2842	17.0		
970.1750 keV		174.3988	12.7		
		204.1050	13.9		
		208.3662	57.4		
		228.4838	37.1		
		281.7868	14.2		
		319.0210	10.5		
		327.6829	18.1		
		378.5036	29.9		
		413.6637	17.5		
		418.5388	21.72		
^{177g}Lu	6.647 d	112.9498	6.23	^{176}Lu(d,p)	4848.324
β-: 100%		**208.3662**	10.41	^{177m}Lu decay	
^{176m}Lu	3.635 h	**88.361**	8.9	^{175}Lu(d,p)	4063.404
β-: 100%				^{176}Lu(d,pn)	− 2224.566
123.014 keV					
^{174g}Lu	3.31 y	**1241.847**	5.14	^{175}Lu(d,p2n)	− 9891.27
ε: 100%				^{176}Lu(d,p3n)	− 16,179.24
				^{174m}Lu decay	
^{173}Lu	1.37 y	78.63	11.9	^{175}Lu(d,p3n)	− 16,651.87
ε: 100%		100.724	5.24	^{176}Lu(d,p4n)	− 22,939.84
		272.105	21.2	^{173}Hf decay	− 18,903.3
^{172}Lu	6.70 d	**181.525**	20.6	^{175}Lu(d,p4n)	− 24,868.12
ε: 100%		203.433	5.02	^{176}Lu(d,p5n)	− 31,156.1
		697.300	6.1		
		810.064	16.6		
		900.724	29.8		
		912.079	15.3		
		1093.63	63		
^{171}Lu	8.24 d	667.422	11.2	^{175}Lu(d,p5)	− 31,847.03
ε: 100%		**739.793**	48.7	^{176}Lu(d,p6)	− 38,135.0
				^{171}Hf decay	− 35,026.4
^{169}Yb	32.018 d	109.77924	17.39	^{175}Lu(d,2p6n)	− 44,658.15
ε: 100%		130.52293	11.38	^{176}Lu(d,2p7n)	− 50,946.12
		177.21307	22.28	^{169}Hf decay	− 51,883.5
		197.95675	35.93	^{169}Lu decay	− 47,733.5
		307.73586	10.05		

Reduce Q-values for emission of clustered particles: pn → d + 2.2 MeV, p2n → t + 8.5 MeV, 2pn → ^{3}He + 7.7 MeV, 2p2n → α + 28.3 MeV

The Q-values shown in Table 1 refer to formation of the ground state. Decrease Q-values for isomeric states with level energy of the isomer

Table 2 (continued) Abundance of isotopes in natural Lu: ^{175}Lu-97.401%, ^{176}Lu-2.599%

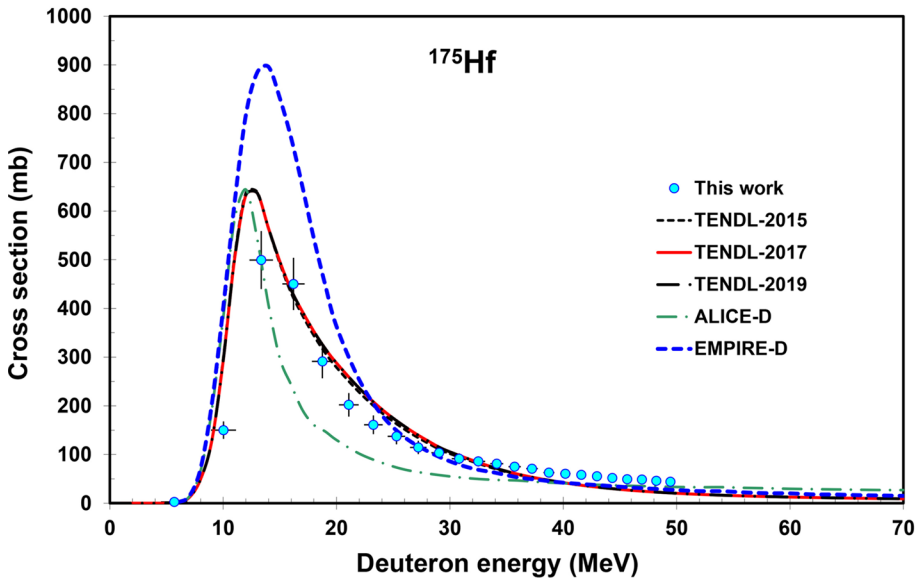

Fig. 2 Experimental and theoretical excitation functions for the ^{nat}Lu(d,x)^{175}Hf reaction

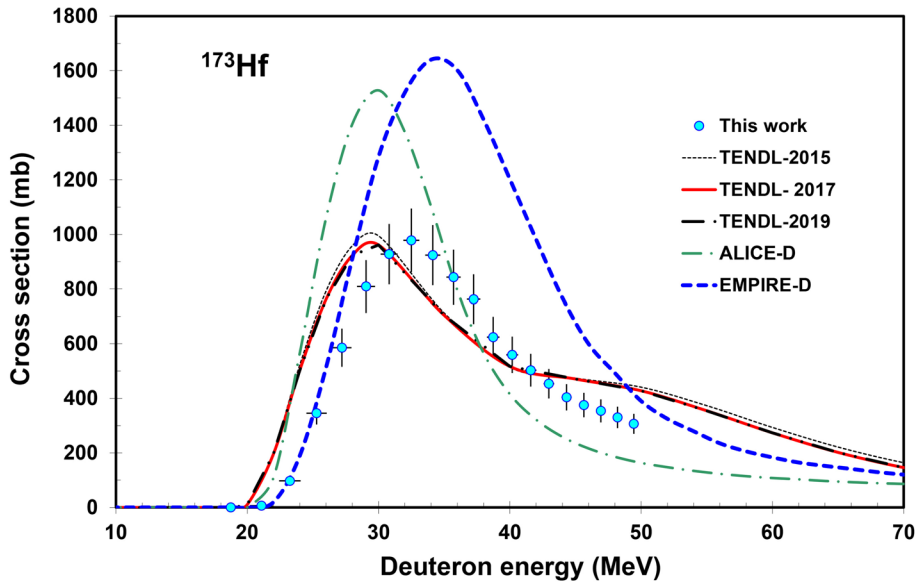

Fig. 3 Experimental and theoretical excitation functions for the ^{nat}Lu(d,x)^{173}Hf reaction

^{nat}Lu(d,x)^{175}Hf reaction

The radionuclide ^{175}Hf has a long, 70-day half-life and only one intense gamma-line at $E_\gamma = 343.4$ keV ($I_\gamma = 84\%$). ^{175}Hf is produced directly in (d,xn) reactions. Data are shown in Fig. 2 together with the result of TALYS calculation taken from TENDL-2017, -2019 data libraries (marginally difference with TENDL-2015) and results of ALICE-D and EMPIRE-D calculations. Our experimental data points fit well on the TENDL curves, except the maximum. Both EMPIRE and ALICE fail to give an acceptable approximation.

^{nat}Lu(d,x)^{173}Hf reaction

The radionuclide ^{173}Hf ($T_{1/2} = 23.6$ h) can be produced directly in (d,xn) reactions. This radionuclide has several intense independent gamma-lines. The cross sections were determined by using the $E_\gamma = 123.7$ keV ($I_\gamma = 83\%$) gamma-line considered to be interference free and confirmed by the results of the other three intense gamma-lines ($I_\gamma > 10\%$). Data are shown in Fig. 3 together with the result of the TALYS, ALICE-D and EMPIRE-D calculations. Some energy shifts of the two TENDL predictions can be observed but the prediction of the energy dependent behavior and

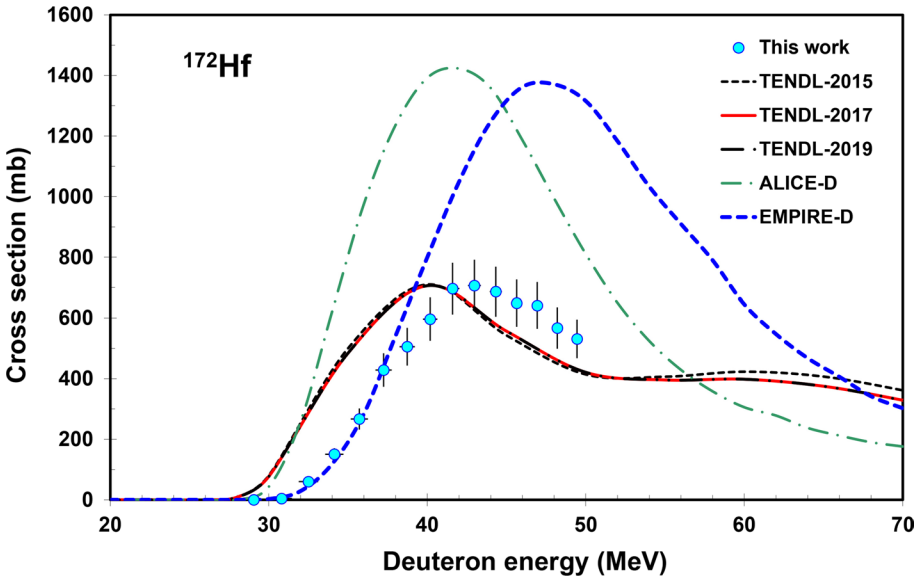

Fig. 4 Experimental and theoretical excitation functions for the ^{nat}Lu(d,x)^{172}Hf reaction

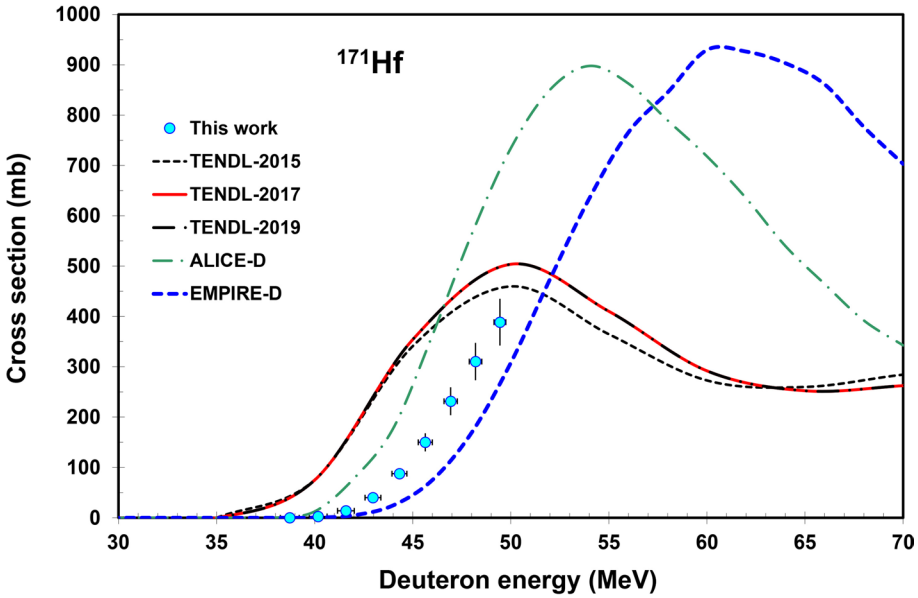

Fig. 5 Experimental and theoretical excitation functions for the ^{nat}Lu(d,x)^{171}Hf reaction

maximum cross section value are good. The ALICE-D and EMPIRE-D codes overestimate almost twice the experimental data.

^{nat}Lu(d,x)^{172}Hf reaction

The long-lived ^{172}Lu (1.87 y) radioisotope is produced via ^{175}Lu(d,5n) and ^{176}Lu(d,6n) reactions. The cross sections were determined by using the most abundant 125.81 keV line among the few strong gamma lines. Comparing with TENDL predictions the agreement in magnitude is good, but the excitation functions (the 2017 and 2019 results are marginally different from the 2015 values) are shifted systematically by 2–3 MeV to the low energy (Fig. 4). The ALICE-D and EMPIRE-D codes overestimate the experiment twice at the maximum, and the ALICE-D predictions are shifted to lower energy.

^{nat}Lu(d,x)^{171}Hf reaction

The measured cross sections of ^{171} Lu (12.1 h) are based on the 347.20 keV (6% per decay) gamma-line. The absolute intensities of gamma-lines following the decay of ^{171}Hf are still under question. The gamma-ray intensities of this reaction product available in different references are all relative. The latest recommendation found in the Nuclear Data Sheets [24] says that the relative intensities (see Table 2) should be multiplied by 0.055 to get absolute intensities if one makes

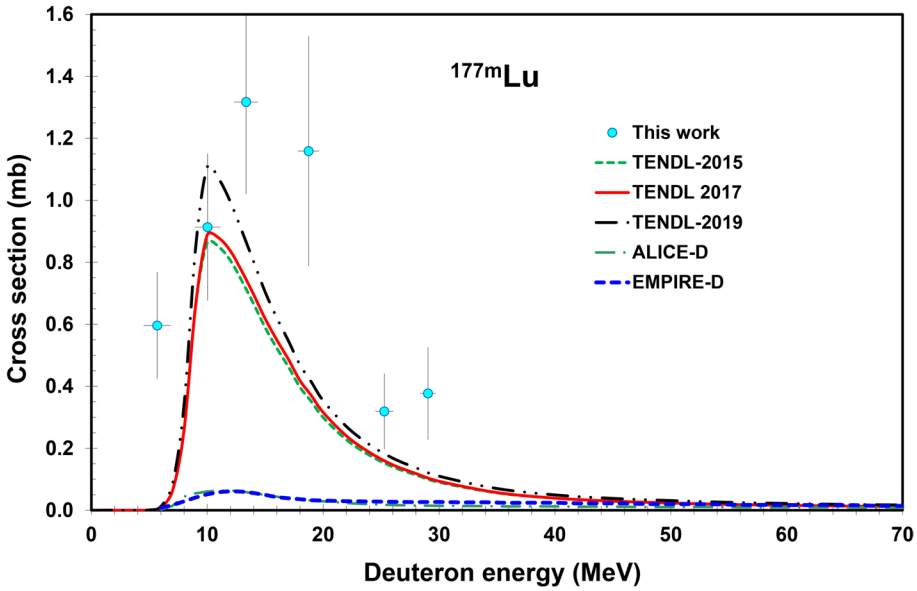

Fig. 6 Experimental and theoretical excitation functions for the ^{nat}Lu(d,x)^{177m}Lu reaction

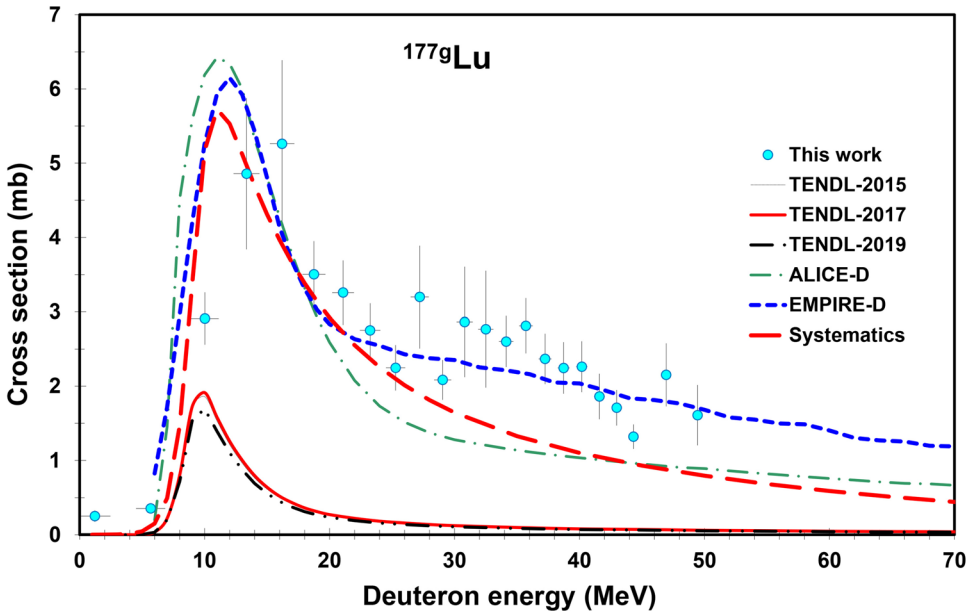

Fig. 7 Experimental and theoretical excitation functions for the ^{nat}Lu(d,x)^{177g}Lu reaction

an assumption that the ground state of Lu is not fed by β^+-decay. According to the present data the ground state is fed by 0.007% β^+-decay, hence the multiplication factor should be a little less.

We have used factor of 0.04 (see values in Table 2) in the cross section evaluation process (which can be corrected according to new valuations in the future) to get a similar difference between our values and the EMPIRE prediction (good threshold) as for ^{171}Lu (Fig. 12), where the contribution of parent ^{171}Hf is dominating. The multiplication factor has been normalized to 100% for the 469.3 keV γ-line. The TENDL and ALICE-D curves are shifted to lower energy (Fig. 5). There is large difference in magnitude between the theoretical data sets near the maximum. Our experimental data can be adapted when more precise decay data are agreed on, but with the present values our experimental results are between the EMPIRE-D and the ALICE-D calculations.

^{nat}Lu(d,x)^{177m}Lu and ^{nat}Lu(d,x)^{177g}Lu reactions

The ^{177m}Lu (160.44 d, 23/2-, IT: 21.4%) and ^{177g}Lu (6.647 d) states are produced only via the ^{176}Lu(d,p) reaction but results are expressed for ^{nat}Lu. For calculation of the cross section of the ^{177m}Lu the highest energy (lowest background) independent γ-line (418.5388 keV) was used, but

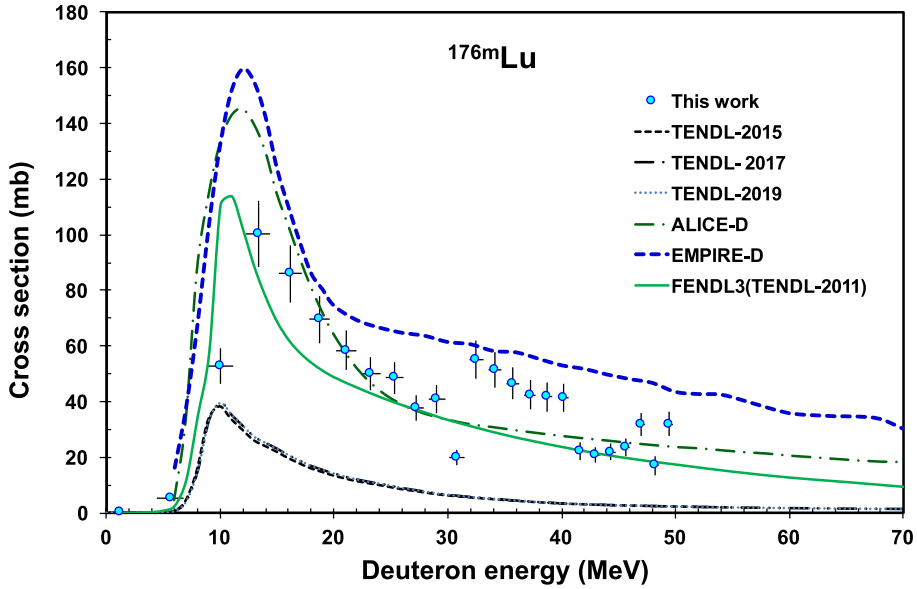

Fig. 8 Experimental and theoretical excitation functions for the ^{nat}Lu(d,x)^{176m}Lu reaction

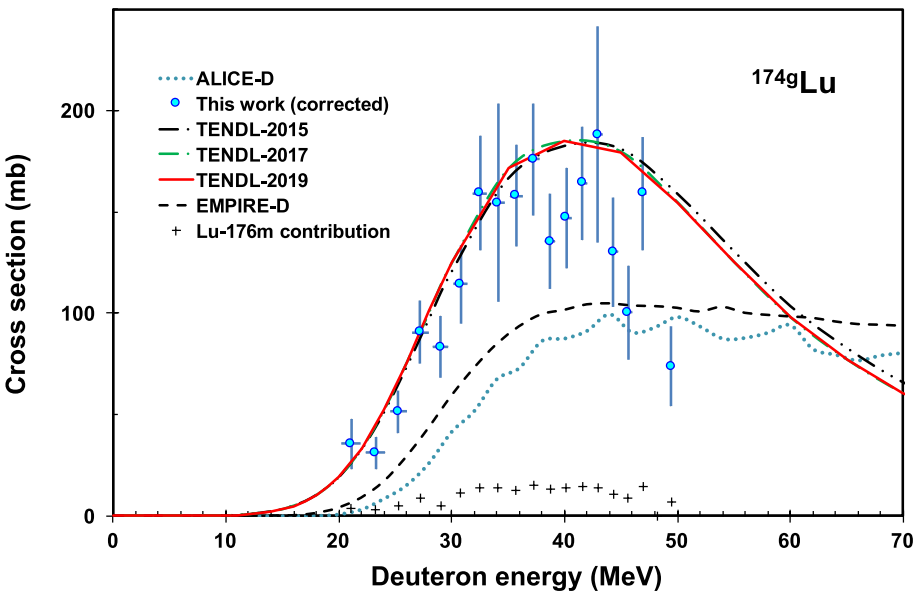

Fig. 9 Experimental and theoretical excitation functions for the ^{nat}Lu(d,x)^{174g}Lu reaction (corrected for ^{174m}Lu contribution)

under our measuring circumstances only poor statistics could be obtained (Fig. 6).

The ^{177g}Lu was identified through its 208.3662 keV γ-line. This line is also present in the β^- decay of ^{177m}Lu, but its contribution can be neglected due to the low cross section for its production and the low activity because of its long half-life. Although, in principle the measured cross sections for ^{177g}Lu are cumulative, the formation through the limited IT (24.1%) of the low induced activity ^{177m}Lu is negligible under our measuring conditions (cooling time for measurement of ground state is short compared to the long-half-life of metastable state) (Fig. 7).

The underestimation of the ^{177m}Lu experimental data by the standard EMPIRE-D and ALICE-D prediction is very significant, while the TENDL is about 40% lower. It is remarkable that the ALICE-D and EMPIRE-D can give an acceptable prediction for the (d,p) reaction leading to ^{177g}Lu while the predicted values of the TENDL libraries are significantly lower (Figs. 6, 7).

^{nat}Lu(d,x)^{176m}Lu reaction

The cross sections for formation of ^{176m}Lu, (3.635 h, 99.905% β^-, 1^-) were obtained through its 88.361 keV

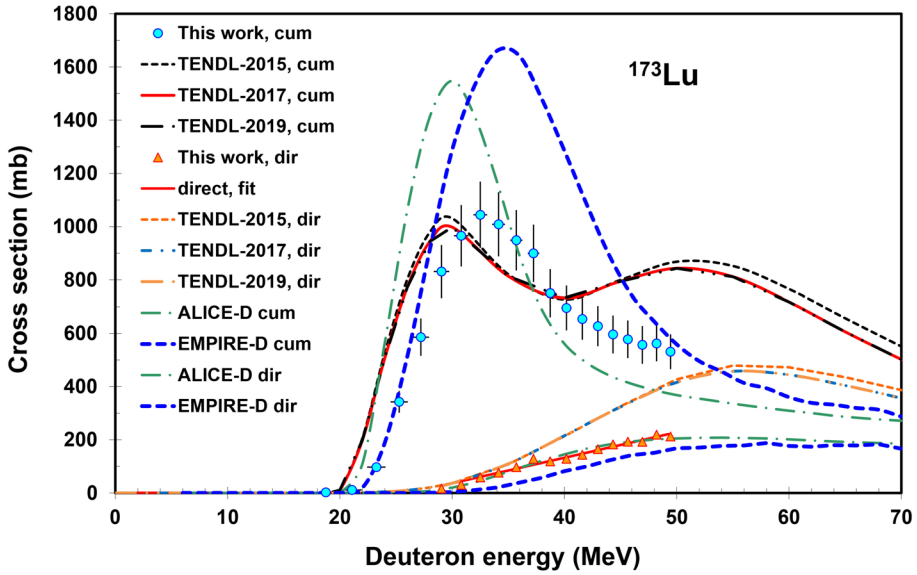

Fig. 10 Experimental and theoretical excitation functions for the ^{nat}Lu(d,x)^{173}Lu reaction

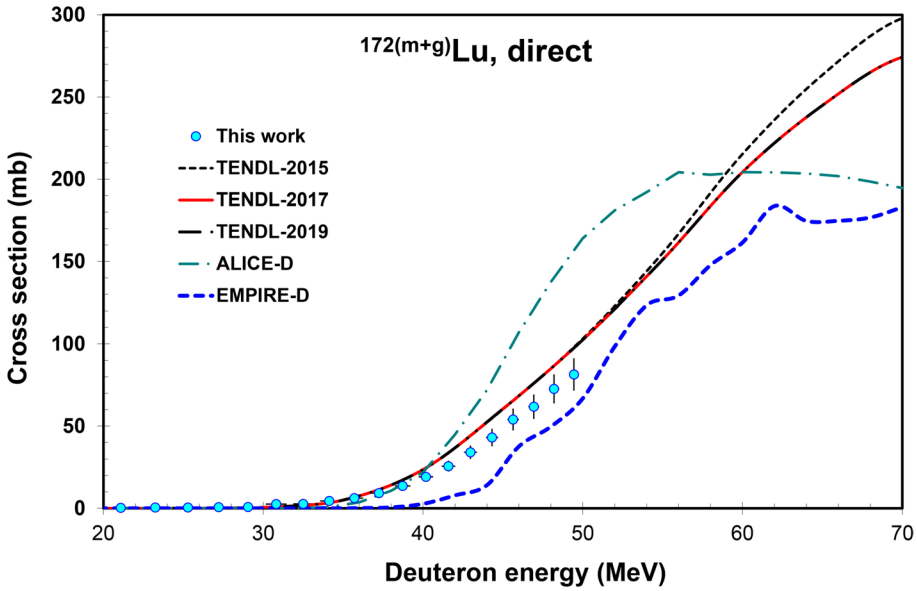

Fig. 11 Experimental and theoretical excitation functions for the ^{nat}Lu(d,x)^{172}Lu reaction

γ-line (Fig. 8). The contribution from same energy γ-line of the quasi-stable ^{176g}Lu (3.76×10^{10} y) can be neglected and it is also the case for the low abundance γ-line with similar energy of ^{177m}Lu (160.44 d, 88.4 keV, 0.037%). As for the previous reaction the TENDL data for the process where emission of a proton is involved, are very low (Fig. 8). The best approximation is given by the ALICE-D. In Fig. 8 also the results of systematics based on the TENDL-2011 on-line library, which was involved in the FENDL-3 database, is presented. This prediction gives also a good approximation of the experimental data, especially from the point of view of the maximum value.

^{nat}Lu(d,x)^{174g}Lu reaction

The ^{174}Lu has two long-lived states, the ^{174m}Lu (142 d, (6-) IT: 99.38%) metastable state and the ^{174g}Lu (3.31 y) ground state. We obtained cross section data for direct production of the ground state (Fig. 9). Taking into account the predicted cross sections for formation of ^{174m}Lu, the decay data and the time of the irradiation and the measurements of the ^{174g}Lu spectra (see Table 1), the contribution from the decay of the metastable state is very low compared with the actual uncertainties, but the experimental curve was corrected with it. Agreement with the TENDL results is acceptable, but in

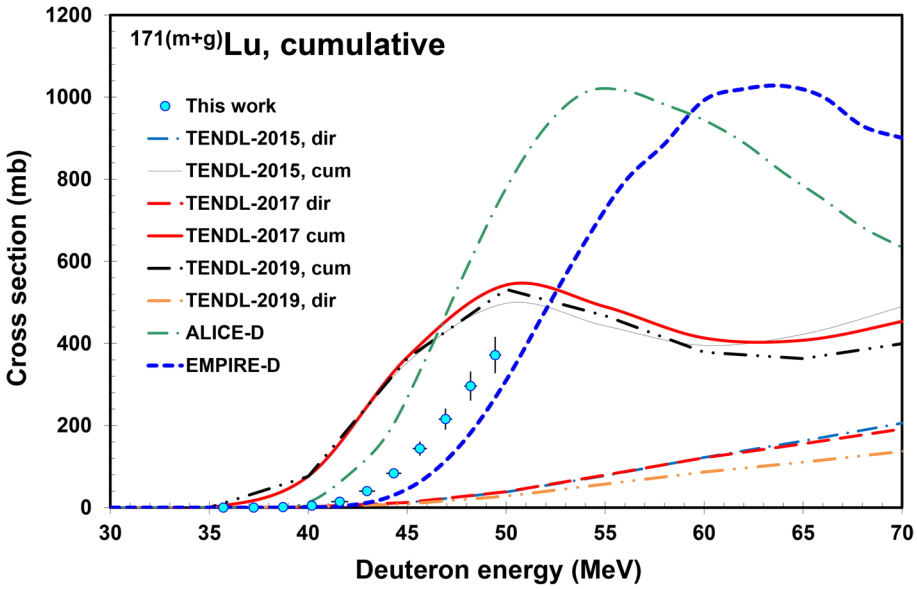

Fig. 12 Experimental and theoretical excitation functions for the ^{nat}Lu(d,x)^{171}Lu(cum) reaction

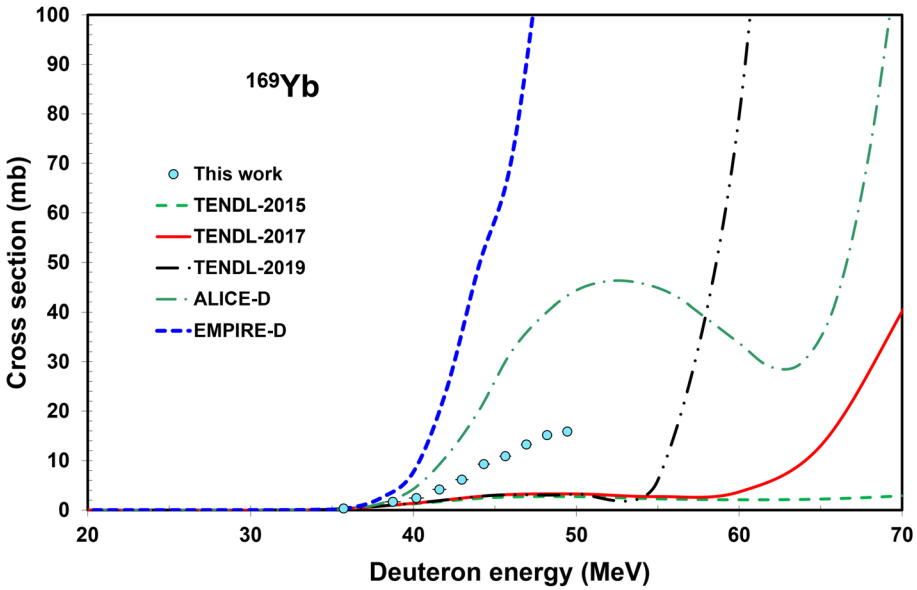

Fig. 13 Experimental and theoretical excitation functions for the ^{nat}Lu(d,x)^{169}Yb reaction

case of ALICE-D and EMPIRE-D the underestimation is significant (Fig. 9).

^{nat}Lu(d,x)^{173}Lu reaction

The ^{173}Lu (1.37 y) is produced directly and through the decay of its ^{173}Hf parent (23.6 h). We measured cumulative production cross section of ^{173}Lu from spectra collected after nearly complete decay of the parent. We deduce cross section data also for direct production by subtracting the contribution of the ^{173}Hf decay (Fig. 10). The magnitudes of theoretical results are very different both for the direct and for the cumulative production (Fig. 10), only the ALICE-D direct prediction agrees very well with our experimental data corrected for the ^{173}Hf decay.

^{nat}Lu(d,x)^{172}Lu reaction

The ground-state of ^{172}Lu (6.70 d) is produced directly, through the decay of its short-lived metastable state (3.7 min, IT: 100%) and through the decay of its long-lived ^{172}Hf parent (1.87 y, ε: 100%). The cross sections were measured from spectra measured a few hours after EOB, in which the effect of decay of ^{172}Hf for production of ^{172}Lu is very low, but has been taken into account. The measured cumulative cross sections for the direct production cross section (m + g)

Table 3 Cross sections of deuteron induced reactions on lutetium for production of ^{171}Hf,^{172}Hf, ^{173}Hf and ^{175}Hf radionuclei

E	dE	^{171}Hf, direct		^{172}Hf, direct		^{173}Hf, direct		^{175}Hf, direct	
		σ	dσ	σ	dσ	σ	dσ	σ	dσ
MeV		mb							
49.4	0.3	388.7	46.5	531.2	63.6	306.5	36.6	44.1	5.4
48.2	0.3	310.4	37.1	567.1	68.2	330.0	39.4	46.1	5.6
46.9	0.3	231.5	27.7	641.4	76.8	354.0	42.2	48.6	5.9
45.6	0.4	149.9	18.0	649.0	77.7	375.4	44.8	49.3	6.0
44.3	0.4	87.6	10.6	686.6	82.2	403.8	48.2	51.7	6.2
43.0	0.4	40.0	4.9	706.5	85.1	453.5	54.1	55.5	6.7
41.6	0.4	13.8	1.9	696.7	85.0	503.1	60.0	58.3	7.0
40.2	0.5	2.7	0.6	596.4	71.3	559.4	66.7	60.6	7.3
38.7	0.5			505.5	62.2	624.3	74.4	62.8	7.6
37.2	0.5			428.6	55.3	762.8	90.9	70.9	8.5
35.7	0.5			266.8	34.9	843.3	100.5	74.9	9.0
34.1	0.6			150.4	19.9	923.9	110.1	81.1	9.7
32.5	0.6			60.2	11.4	978.1	116.6	85.8	10.3
30.8	0.6			4.2	2.2	927.5	110.6	91.3	10.9
29.0	0.7					809.1	96.5	103.5	12.4
27.2	0.7					585.5	69.8	114.5	13.7
25.3	0.8					345.4	41.2	137.3	16.4
23.2	0.8					97.6	11.7	161.1	19.2
21.1	0.9					6.5	0.8	202.0	24.1
18.7	0.9					0.3	0.1	291.2	34.7
16.2	1.0							450.4	53.7
13.4	1.0							499.4	59.5
10.0	1.1							150.1	17.9
5.7	1.2							2.6	0.3

are shown in Fig. 11. The agreement with description of the theoretical codes is moderate, but disagreement especially in shape and energy shift of the effective threshold can be noted, especially the TALYS calculations are more consistent with our experimental data than the both other codes.

^{nat}Lu(d,x)^{171}Lu(cum) reaction

The cross sections for cumulative production of the ground-state of ^{171}Lu (8.24 d) are shown in Fig. 12. It includes the direct production, the decay of the short lived isomeric state (79 s, IT: 100%) and the decay of the ^{171}Hf parent (12.1 h, ε: 100%). The TENDL-2017, 2019 (and TENDL-2015 with slightly larger values above 43 MeV) and ALICE-D cumulative data are shifted to lower energy because of the contribution of ^{171}Hf that already showed this difference between experiment and theory (Fig. 5). The ^{171}Hf contribution has not been subtracted because of the uncertain intensity data of ^{171}Hf. The shape, the effective threshold and the magnitude of the results of the different theoretical codes differ significantly. The best agreement is seen with the prediction of the EMPIRE-D code.

^{nat}Lu(d,x)^{169}Yb reaction

The practical threshold of 36 MeV indicates that clustered emission is involved in formation of ^{169}Yb and that in the investigated energy range (up to 50 MeV) the predominant reaction is ^{nat}Lu(d,αxn) (see Table 2). The experimental data are significantly higher than the TENDL-2017, 2019 prediction, as well as significantly lower compared to ALICE-D and EMPIRE-D (Fig. 13).

Integral yields

Integral yields were calculated from excitation functions constructed by an analytical fit to our experimental cross section data points (Fig. 14). The so-called physical integral yield [12]. Otuka [13] was calculated (yield at EOB for an instantaneous irradiation, i.e. no decay corrections).

Table 4 Cross sections of deuteron induced reactions on lutetium for production of $^{171(m+g)}$Lu, $^{172(m+g)}$Lu, ^{173}Lu and ^{174g}Lu radionuclei

E	dE	$^{171(m+g)}$Lu, cum		$^{172(m+g)}$Lu, direct		^{173}Lu, cum		^{173}Lu, direct		^{174g}Lu, direct	
		σ	dσ	σ	dσ	σ	dσ	σ	dσ	σ	dσ
MeV		mb									
49.4	0.3	372	44	81.4	9.8	531.0	65.4	212.6	53.2	73.8	1.6
48.2	0.3	296	35	72.6	8.8	562.3	67.2	219.4	56.8		
46.9	0.3	216	26	61.8	7.4	556.6	70.8	192.2	58.3	159.0	2.2
45.6	0.4	144	17	54.0	6.6	577.7	70.6	193.0	61.1	100.3	0.0
44.3	0.4	84	10	43.0	5.3	595.6	71.1	182.8	64.5	130.2	1.3
43.0	0.4	40	5	34.1	4.1	627.0	75.2	164.8	70.7	188.1	1.7
41.6	0.4	15	2	25.6	3.3	654.2	78.1	143.3	77.0	164.0	1.9
40.2	0.5	4.7	0.6	19.2	2.6	695.0	83.8	128.4	84.7	147.1	2.3
38.7	0.5	1.2	0.2	13.6	2.0	750.3	90.1	118.9	93.9	135.3	2.2
37.2	0.5	0.14	0.08	9.2	1.2	899.6	107.8	128.4	114.4	175.9	2.4
35.7	0.5	0.22	0.08	6.1	1.0	948.7	113.5	97.1	125.7	157.8	2.8
34.1	0.6			4.5	0.6	1008.7	120.4	76.6	137.3	154.4	2.6
32.5	0.6			2.7	0.4	1044.3	124.8	58.4	145.1	159.2	2.8
30.8	0.6			2.6	0.9	965.7	115.4	31.3	137.4	114.4	2.9
29.0	0.7			0.7	0.1	831.4	99.4	16.4	119.8	83.4	2.1
27.2	0.7			0.7	0.2	585.6	70.1			90.7	3.2
25.3	0.8			0.5	0.2	342.5	40.9			51.6	2.2
23.2	0.8			0.5	0.1	97.3	11.7			31.0	2.8
21.1	0.9			0.3	0.2	11.4	1.7			35.5	3.3
18.7	0.9					2	1				

Review of production options of ^{177}Lu, ^{175}Hf and ^{172}Hf with charged particle nuclear reactions

The new experimental data provide a basis for improved model calculations and for optimization various charged particle production routes. Concerning applications in nuclear medicine among the investigated radioisotopes the ^{177}Lu (variety of therapeutic procedures, theranostic), ^{176m}Lu (in SPECT, to image the distribution of lutetium), ^{175}Hf for nuclear-medical investigations and for off-line chemical studies of Group IV homologs, ^{172}Hf-^{172}Lu (radionuclide generator for industrial radiotracer applications and for pre-clinical bio-distribution studies), ^{169}Yb (brachytherapy, as an alternative to ^{125}I) have established practical applications. In the following chapters we compare the production yields of the deuteron induced reactions with other charged particle production routes. Of course for production of the above mentioned radioisotopes many other parameters should be taken into account.

^{177}Lu production

Non-charged particle production routes

The widely used, non-charged particle production routes use nuclear reactors and high intensity gamma sources [25]. In case of ^{176}Yb(n,γ)-^{177}Yb-^{177}Lu indirect route the product has high specific activity and it is close to carrier free. In case of direct production ^{177}Lu(n,γ)^{177}Lu the product is not carrier free, but may still be produced in very high specific activity. By using the ^{nat}Hf(γ,x) ^{177}Lu reaction via high energy bremsstrahlung photons hundreds of mCi of ^{177}Lu activity can be obtained on targets from 10 g enriched hafnium-oxide [26].

Charged particle induced reactions

The production yields of ^{nat}Yb(d,x)^{177}Lu, ^{nat}Hf(p,x)^{177}Lu, ^{nat}Hf(d,x)^{177}Lu, ^{nat}Lu(p,x) ^{177}Lu, ^{nat}Lu(d,x)^{177}Lu and ^{nat}Yb(α,x)^{177}Lu routes are collected together for comparison (Fig. 15), The calculated integral yields are based on experimental data in the literature except ^{nat}Lu(p,x) where experimental data are missing therefore the TENDL-2019 data were used

The production yield of ^{nat}Yb(d,x)^{177}Lu reaction is based on experimental data reported by Manenti [27], Hermanne [28], Tarkanyi [29] and Tarkanyi [30], Khandaker [31], the ^{nat}Hf(p,x) on [32], the ^{nat}Hf(d,x) on [33], ^{nat}Lu(d,x) [this work] and the ^{nat}Yb(α,x) on [34, 35].

As it is seen from Fig. 15, the best way to produce ^{177}Lu is the Yb + d reaction, if a high energy accelerator is available.

Table 5 Cross sections of deuteron induced reactions on lutetium for production of ^{176m}Lu, ^{177m}Lu, ^{177g}Lu and ^{169}Yb radionuclei

E	dE	^{176m}Lu, direct		^{177m}Lu, direct		^{177g}Lu, cum		^{169}Yb, cum	
		σ	dσ	σ	dσ	σ	dσ	σ	dσ
(MeV)		mb							
49.4	0.3	32.0	4.5			1.86	0.31	15.9	1.9
48.2	0.3	17.1	3.4			2.26	0.34	15.2	1.8
46.9	0.3	31.7	4.2			2.25	0.35	13.3	1.6
45.6	0.4	23.5	3.3			2.37	0.34	10.9	1.3
44.3	0.4	22.0	2.9			2.81	0.37	9.3	1.1
43.0	0.4	20.7	2.8			2.60	0.34	6.2	0.7
41.6	0.4	22.3	3.2			2.77	0.79	4.2	0.5
40.2	0.5	41.4	5.1			2.86	0.74	2.4	0.3
38.7	0.5	41.6	5.2			2.09	0.27	1.7	0.3
37.2	0.5	42.5	5.2			3.20	0.69		
35.7	0.5	46.6	5.8			2.25	0.31	0.3	0.1
34.1	0.6	51.6	6.3			2.75	0.36		
32.5	0.6	55.1	6.7			3.26	0.43		
30.8	0.6	20.1	2.8			3.50	0.45		
29.0	0.7	41.0	5.1	0.38	0.15	5.26	1.13		
27.2	0.7	37.6	4.6			4.86	1.02		
25.3	0.8	48.5	5.9	0.32	0.12	2.91	0.35		
23.2	0.8	50.1	6.0			0.35	0.05		
21.1	0.9	58.5	7.0			0.25	0.08		
18.7	0.9	69.6	8.3	1.16	0.37				
16.2	1.0	86.1	10.3						
13.4	1.0	100.2	12.0	1.32	0.30				
10.0	1.1	52.8	6.4	0.91	0.24				
5.7	1.2	5.4	0.7	0.60	0.17				

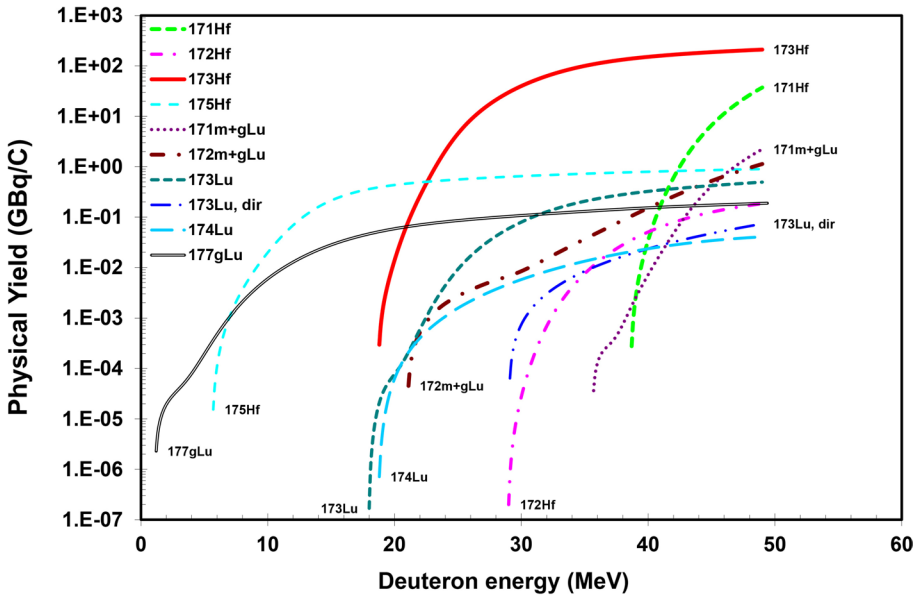

Fig. 14 Integral thick target yields for the formation of the investigated radioisotopes of hafnium, lutetium and ytterbium as a function of incident energy

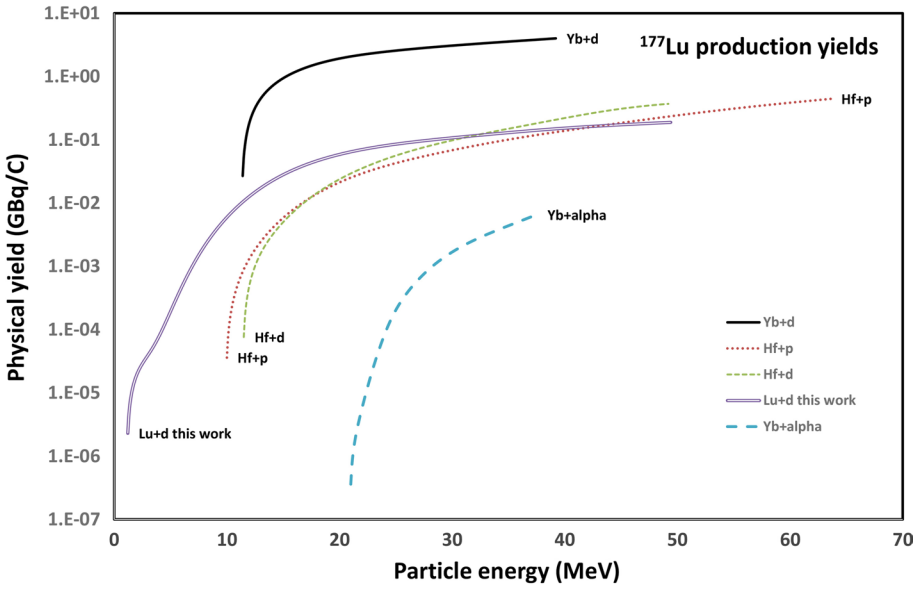

Fig. 15 Integral yields for production of ^{177}Lu

In the case of a compact cyclotron with deuteron energies not higher than 10 MeV the Lu + d reaction (this work) gives an acceptable alternative.

^{175}Hf production

The ^{175}Hf can be produced via (p,xn) and (d,xn) reaction on ^{nat}Lu or on enriched ^{175}Lu(97.41%) and ^{176}Lu(2.59%) or on (α,xn) reaction on ^{nat}Yb. Experimental data are available for ^{nat}Lu(p,x)^{175}Hf [36] (only cross section), ^{nat}Lu(d,x)^{175}Hf (this work) and ^{nat}Yb(α,xn)^{175}Hf [34] reactions (Fig. 16). The product in all cases is no carrier added, in case of ^{175}Lu(p,n) reaction the product is of high specific activitz. By using natural Lu target the deuteron route is much more productive. By using highly enriched targets the yield of the ^{176}Lu(p,2n) is higher. Comparing the proton and deuteron induced reactions on Lu one can conclude that the deuteron reaction has much higher cross sections, but at higher energies, which excludes compact cyclotrons with deuteron option under 10 MeV.

^{172}Hf production

We have compared the charged particle production routes for ^{172}Hf/^{172}Lu generator in our previous paper [2]. Here we reproduce the figure of production yields completed with Lu + d reaction. In accordance with Fig. 17 in the low energy range the Yb + α, at high energies the Lu + p reactions are

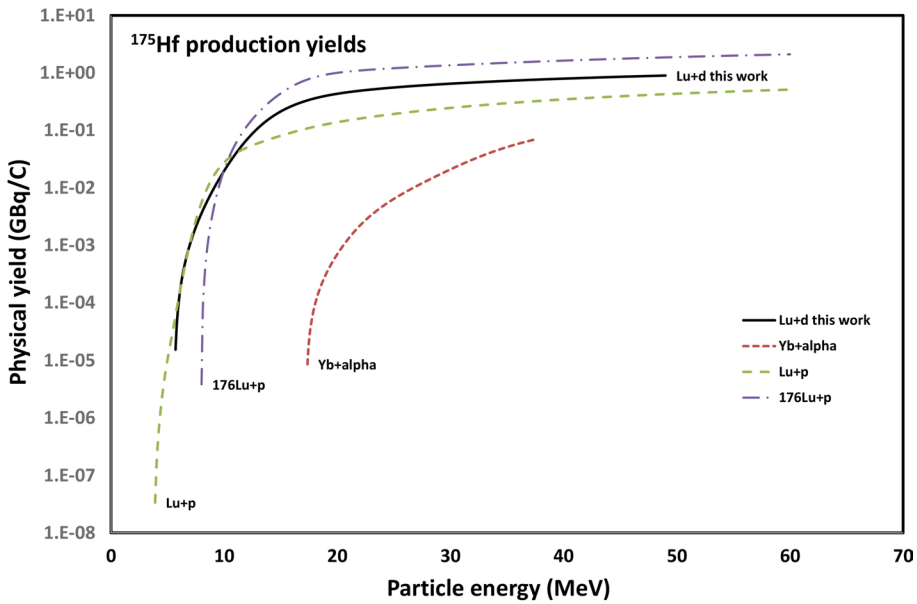

Fig. 16 Integral yields for production of ^{175}Hf

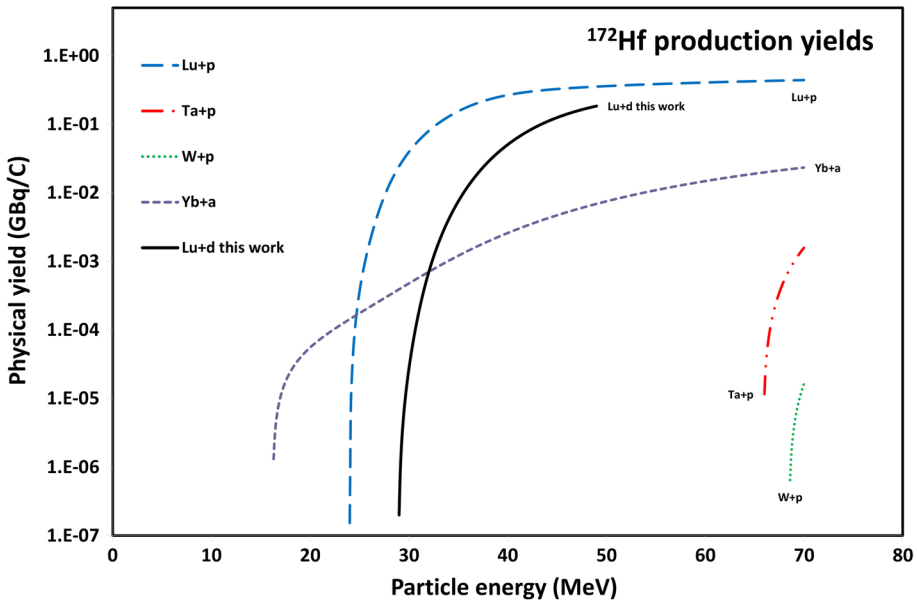

Fig. 17 Integral yields for production of ^{172}Hf

the more productive routes. The calculated integral yields are based on experimental data Tarkanyi 2017 [37], Michel 2002 [38], Titarenko 2011 [39].

Summary and conclusions

In the frame of a systematic study of activation cross sections of deuteron induced reactions we report experimental cross sections for the ^{nat}Lu(d,x) ^{171,172,173,175}Hf, ^{171,172,173,174g,176m,177m,177g}Lu and ^{169}Yb reactions up to 50 MeV. No earlier experimental data were found in the literature. The experimental data were compared with the results of a priori model calculations performed with the EMPIRE-D, ALICE-IPPE-D and TALYS codes (available in TENDL-2015, TENDL-2017 and TENDL-2019 on-line libraries) using reference input parameters. The descriptions of the shape and the absolute values of the excitation functions by the theoretical calculations is only partly successful, especially observed energy shifts, shape and magnitude disagreements underline the importance of the experimental data. There are only marginal differences on data of predictions of the applied latest versions.

Concerning the use of deuteron induced nuclear reactions for production of medically relevant ^{177}Lu, ^{175}Hf and ^{172}Hf, in case of ^{177}Lu the product is carrier added. Yield calculations based on excitation functions for production of the ^{175}Hf show that the ^{nat}Lu + d yield is the highest comparing to ^{nat}Lu + p and Yb + α routes, but in the case of enriched ^{176}Lu target the proton induced reaction gives higher yield. By comparing the production routes of ^{172}Hf via Lu + p, Lu + d, Yb + α, Ta + p and W + p reactions up to 70 MeV, we clearly see that the Lu + d yields are also high and at higher energies almost as high as those for the Lu + p route.

Acknowledgements Open access funding provided by Institute for Nuclear Research. The authors acknowledge the support of the respective institutions and the accelerator staffs for providing the beam time and experimental facilities.

Open Access This article is licensed under a Creative Commons Attribution 4.0 International License, which permits use, sharing, adaptation, distribution and reproduction in any medium or format, as long as you give appropriate credit to the original author(s) and the source, provide a link to the Creative Commons licence, and indicate if changes were made. The images or other third party material in this article are included in the article's Creative Commons licence, unless indicated otherwise in a credit line to the material. If material is not included in the article's Creative Commons licence and your intended use is not permitted by statutory regulation or exceeds the permitted use, you will need to obtain permission directly from the copyright holder. To view a copy of this licence, visit http://creativecommons.org/licenses/by/4.0/.

References

1. Takács S, Tárkányi F, Hermanne A, Adam-Rebeles R (2016) Investigation of cross sections of deuteron induced nuclear reactions on natural lutetium. Paper presented at the International conference on radioanalytical and nuclear chemistry. RANC 2016, Budapest, Hungary
2. Tarkanyi F, Hermanne A, Ditroi F, Takacs S, Ignatyuk AV (2018) Activation cross-sections of proton induced reactions on Hf-nat in the 38–65 MeV energy range: production of Lu-172 and of Yb-169. Nucl Instrum Methods Phys Res Sect B 427:20–37. https://doi.org/10.1016/j.nimb.2018.04.036
3. Tárkányi F, Takács S, Gul K, Hermanne A, Mustafa MG, Nortier M, Oblozinsky P, Qaim SM, Scholten B, Shubin YN, Youxiang Z (2001) Charged particles cross-sections database for medical

radioisotope production. Beam monitors reactions IAEA. http://www-nds.iaea.org/medical
4. Székely G (1985) Fgm—a flexible gamma-spectrum analysis program for a small computer. Comput Phys Commun 34(3):313–324. https://doi.org/10.1016/0010-4655(85)90008-6
5. Canberra (2000). http://www.canberra.com/products/radiochemistry_lab/genie-2000-software.asp. 2013
6. Tárkányi F, Szelecsényi F, Takács S (1991) Determination of effective bombarding energies and fluxes using improved stacked-foil technique. Acta Radiol Suppl 376:72
7. Kinsey RR, Dunford CL, Tuli JK, Burrows TW (1997) Capture gamma-ray spectroscopy and related topics, vol 2 (NUDAT 2.6 http://www.nndc.bnl.gov/nudat2/). Springer Hungarica Ltd, Budapest
8. Q-value calculator (2003) NNDC. Brookhaven National Laboratory. http://www.nndc.bnl.gov/qcalc
9. Andersen HH, Ziegler JF (1977) Hydrogen stopping powers and ranges in all elements. In: Ziegler JF (ed) The stopping and ranges of ions in matter, vol 3. Pergamon Press, New York
10. Tárkányi F, Takács S, Gul K, Hermanne A, Mustafa MG, Nortier M, Oblozinsky P, Qaim SM, Scholten B, Shubin YN, Youxiang Z (2001) Beam monitor reactions (Chap 4). Charged particle cross-section database for medical radioisotope production: diagnostic radioisotopes and monitor reactions. In: TECDOC 1211, vol 1211. IAEA
11. International-Bureau-of-Weights-and-Measures (1993) Guide to the expression of uncertainty in measurement, 1st edn. International Organization for Standardization, Genève
12. Bonardi M (1987) The contribution to nuclear data for biomedical radioisotope production from the Milan cyclotron facility. Paper presented at the Consultants Meeting on Data Requirements for Medical Radioisotope Production, Tokyo, Japan
13. Otuka N, Takács S (2015) Definitions of radioisotope thick target yields. Radiochim Acta 103(1):1–6. https://doi.org/10.1515/ract-2013-2234
14. Dityuk AI, Konobeyev AY, Lunev VP, Shubin YN (1998) New version of the advanced computer code ALICE-IPPE. INDC (CCP)-410. IAEA, Vienna
15. Herman M, Capote R, Carlson BV, Oblozinsky P, Sin M, Trkov A, Wienke H, Zerkin V (2007) EMPIRE: nuclear reaction model code system for data evaluation. Nucl Data Sheets 108(12):2655–2715. https://doi.org/10.1016/j.nds.2007.11.003
16. Koning AJ, Rochman D, Kopecky J, Sublet JC, Bauge E, Hilaire S, Romain P, Morillon B, Duarte H, van der Marck S, Pomp S, Sjostrand H, Forrest R, Henriksson H, Cabellos O, Leppanen J, Leeb H, Plompen A, Mills R (2015) TENDL-2015: TALYS-based evaluated nuclear data library. https://tendl.web.psi.ch/tendl_2015/tendl2015.html
17. Koning AJ, Rochman D, Sublet JC, Dzysiuk N, Fleming M, van der Marck S (2019) TENDL: complete nuclear data library for innovative nuclear science and technology. Nucl Data Sheets 155:1–55. https://doi.org/10.1016/j.nds.2019.01.002
18. NuDat2 database (2.6) (2014) National Nuclear Data Center, Brookhaven National Laboratory. http://www.nndc.bnl.gov/nudat2/
19. Tárkányi F, Hermanne A, Takács S, Hilgers K, Kovalev SF, Ignatyuk AV, Qaim SM (2007) Study of the ^{192}Os(d,2n) reaction for, production of the therapeutic radionuclide ^{192}Ir in no-carrier added form. Appl Radiat Isot 65(11):1215–1220. https://doi.org/10.1016/j.apradiso.2007.06.007
20. Hermanne A, Tárkányi F, Takács S, Ditrói F, Baba M, Ohtshuki T, Spahn I, Ignatyuk AV (2009) Excitation functions for production of medically relevant radioisotopes in deuteron irradiations of Pr and Tm targets. Nucl Instrum Methods Phys Res Sect B 267(5):727–736. https://doi.org/10.1016/j.nimb.2008.12.017
21. Belgya T, Bersillon O, Capote R, Fukahori T, Zhigang G, Goriely S, Herman M, Ignatyuk AV, Kailas S, Koning A, Oblozinsky P, Plujko V, Young P (2005) Handbook for calculations of nuclear reaction data: Reference Input Parameter Library. http://www-nds.iaea.org/RIPL-2/. IAEA, Vienna
22. Koning AJ, Rochman D, Sublet JC (2017) TENDL-2017 TALYS-based evaluated nuclear data library. https://tendl.web.psi.ch/tendl_2017/tendl2017.html. 2018
23. Koning AJ, Hilaire S, Duijvestijn MC (2007) TALYS-1.0. Paper presented at the International conference on nuclear data for science and technology, Nice, France,
24. Baglin CM, McCutchan EA (2018) Nuclear data sheets for A = 171. Nucl Data Sheets 151:334–718. https://doi.org/10.1016/j.nds.2018.08.002
25. Dash A, Pillai MRA, Knapp FF (2015) Production of Lu-177 for targeted radionuclide therapy: available options. Nucl Med Mol Imaging 49(2):85–107. https://doi.org/10.1007/s13139-014-0315-z
26. Kazakov AG, Belyshev SS, Ekatova TY, Khankin VV, Kuznetsov AA, Aliev RA (2018) Production of Lu-177 by hafnium irradiation using 55-MeV bremsstrahlung photons. J Radioanal Nucl Chem 317(3):1469–1476. https://doi.org/10.1007/s10967-018-6036-5
27. Manenti S, Groppi F, Gandini A, Gini L, Abbas K, Holzwarth U, Simonelli F, Bonardi M (2011) Excitation function for deuteron induced nuclear reactions on natural ytterbium for production of high specific activity Lu-177 g in no-carrier-added form for metabolic radiotherapy. Appl Radiat Isot 69(1):37–45. https://doi.org/10.1016/j.apradiso.2010.08.008
28. Hermanne A, Takacs S, Goldberg MB, Lavie E, Shubin YN, Kovalev S (2006) Deuteron-induced reactions on Yb: measured cross sections and rationale for production pathways of carrier-free, medically relevant radionuclides. Nucl Instrum Methods Phys Res Sect B 247(2):223–231. https://doi.org/10.1016/j.nimb.2006.03.008
29. Tárkányi F, Ditrói F, Takács S, Hermanne A, Ignatyuk AV (2014) New data on activation cross section for deuteron induced reactions on ytterbium up to 50 MeV. Nucl Instrum Methods Phys Res Sect B 336:37–44
30. Tárkányi F, Ditrói F, Takács S, Hermanne A, Yamazaki H, Baba M, Mohammadi A, Ignatyuk AV (2013) Activation cross-sections of longer lived products of deuteron induced nuclear reactions on ytterbium up to 40 MeV. Nucl Instrum Methods Phys Res Sect B 304:36–48
31. Khandaker MU, Haba H, Otuka N, Usman AR (2014) Investigation of (d, x) nuclear reactions on natural ytterbium up to 24 MeV. Nucl Instrum Methods Phys Res Sect B 335:8–18. https://doi.org/10.1016/j.nimb.2014.05.020
32. Takács S, Tárkányi F, Hermanne A, Rebeles RA (2011) Activation cross sections of proton induced nuclear reactions on natural hafnium. Nucl Instrum Methods Phys Res Sect B 269(23):2824–2834. https://doi.org/10.1016/j.nimb.2011.08.021
33. Takács S, Tárkányi F, Hermanne A, Rebeles RA (2012) Activation cross sections of deuteron-induced nuclear reactions on hafnium (vol 268, pg 3443, 2010). Nucl Instrum Methods Phys Res Sect B 281:98–99. https://doi.org/10.1016/j.nimb.2012.02.023
34. Király B, Tárkányi F, Takács S, Hermanne A, Kovalev SF, Ignatyuk AV (2008) Excitation functions of alpha-particle induced nuclear reactions on natural ytterbium. Nucl Instrum Methods Phys Res Sect B 266(18):3919–3926. https://doi.org/10.1016/j.nimb.2008.07.002
35. Oganessian YT, Karamian SA Yield of Lu-177-m, Hf-178-m2 and Hf-179-m2 isomers in the reaction He-4 + Yb-176. In: Conference on nuclear spectroscopy and nuclear structure, St. Petersburg,

Russia, 1995. Joint Institute for Nuclear Research (JINR), Dubna, p 222
36. Bennett ME, Mayorov DA, Chapkin KD, Alfonso MC, Werke TA, Folden CM (2012) Measurement of the Lu-nat(p, x)Hf-175 excitation function. Nucl Instrum Methods Phys Res Sect B 276:62–65. https://doi.org/10.1016/j.nimb.2012.01.039
37. Tárkányi F, Ditrói F, Takács S, Hermanne A, Király B (2017) Activation cross-section data for alpha-particle induced nuclear reactions on natural ytterbium for some longer lived radioisotopes. J Radioanal Nucl Chem 311(3):1825–1829. https://doi.org/10.1007/s10967-016-5139-0
38. Michel R, Gloris M, Protoschill J, Herpers U, Kuhnhenn J, Sudbrock F, Malmborg P, Kubik P (2002) Cross sections for the production of radionuclides by proton-induced reactions on W, Ta, Pb and Bi from thresholds up to 2.6 GeV. J Nucl Sci Technol 39(sup2):242–245. https://doi.org/10.1080/00223131.2002.10875084
39. Titarenko YE, Batyaev VF, Titarenko AY, Butko MA, Pavlov KV, Florya SN, Tikhonov RS, Zhivun VM, Ignatyuk AV, Mashnik SG, Leray S, Boudard A, Cugnon J, Mancusi D, Yariv Y, Nishihara K, Matsuda N, Kumawat H, Mank G, Gudowski W (2011) Measurement and simulation of the cross sections for the production of Gd-148 in thin W-nat and Ta-181 targets irradiated with 0.4- to 2.6-GeV protons. Phys Atom Nucl 74(4):573–579. https://doi.org/10.1134/s1063778811040193

Publisher's Note Springer Nature remains neutral with regard to jurisdictional claims in published maps and institutional affiliations.